

The potential of discs from a “mean Green function”

A. Trova^{1,2*}, J.-M. Huré^{1,2†} and F. Hersant^{1,2‡}

¹Univ. Bordeaux, LAB, UMR 5804, F-33270 Floirac, France

²CNRS, LAB, UMR 5804, F-33270 Floirac, France

Accepted ???. Received ???

ABSTRACT

By using various properties of the complete elliptic integrals, we have derived an alternative expression for the gravitational potential of axially symmetric bodies, which is free of singular kernel in contrast with the classical form. This is mainly a radial integral of the local surface density weighted by a regular “mean Green function” which depends explicitly on the body’s vertical thickness. Rigorously, this result stands for a wide variety of configurations, as soon as the density structure is vertically homogeneous. Nevertheless, the sensitivity to vertical stratification — the Gaussian profile has been considered — appears weak provided that the surface density is conserved. For bodies with small aspect ratio (i.e. geometrically thin discs), a first-order Taylor expansion furnishes an excellent approximation for this mean Green function, the absolute error being of the fourth order in the aspect ratio. This formula is therefore well suited to studying the structure of self-gravitating discs and rings in the spirit of the “standard model of thin discs” where the vertical structure is often ignored, but it remains accurate for discs and tori of finite thickness. This approximation which perfectly saves the properties of Newton’s law everywhere (in particular at large separations), is also very useful for dynamical studies where the body is just a source of gravity acting on external test particles.

Key words: Accretion, accretion discs — Gravitation — Methods: analytical — Methods: numerical

1 INTRODUCTION

The capability to calculate properly the gravitational potential inside celestial bodies is a longstanding challenge in Astrophysics, mainly due to the difficulty to manage the hyperbolic divergence $1/|\vec{r} - \vec{r}'|$ (a major feature of Newton’s law). The presence of strong inhomogeneities of density and complex geometries or shapes seem less problematic in comparison. For a few special configurations (not always realistic), the potential/density pair is simple and analytical (Mestel 1963; Binney & Tremaine 1987). However, for most realistic matter distributions, a numerical computation of the gravitational potential has to be performed, either from the integral form when accuracy is required (Ambastha & Varma 1983; Hachisu 1986; Stone & Norman 1992; Baruteau & Masset 2008), or from the Poisson equation, when computational time is the limiting factor (Bodo & Curir 1992; Fromang et al. 2004). While most theoretical developments allow to reach any degree of

accuracy, their numerical implementation are usually limited by errors and uncertainties of various origins. A striking illustration is the infinite series representation of the Green function in terms of Legendre polynomials which, although exact, is known to have a (very) low convergence rate inside sources (see e.g. Kellogg 1929; Durand 1953); so, its implementation is often disappointing in practice (Clement 1974; Hachisu 1986). Compact integral expressions, despite singularities, may then be preferred (Cohl & Tohline 1999; Huré & Pierens 2005).

The gravitational potential of discs, starting with galactic discs, has received much attention in the last decades (Mestel 1963; Binney & Tremaine 1987). Even for very simple and academic configurations, new analytic solutions and approximations continue to be produced (Cox & Gómez 2002; Schulz 2009; Vogt & Letelier 2010, 2011; Huré et al. 2011; Bannikova et al. 2011; Schulz 2011), either for establishing theoretical references, or for analysing observations. The problem is far from being solved. Searching for new formulae or techniques aiming at improving the description (in terms of computation time, accuracy, series convergence, singularity avoidance, etc.) of gravitational potentials and forces of celestial bodies is therefore still of relevance today.

* E-mail:audrey.trova@obs.u-bordeaux1.fr

† E-mail:jean-marc.hure@obs.u-bordeaux1.fr

‡ E-mail:franck.hersant@obs.u-bordeaux1.fr

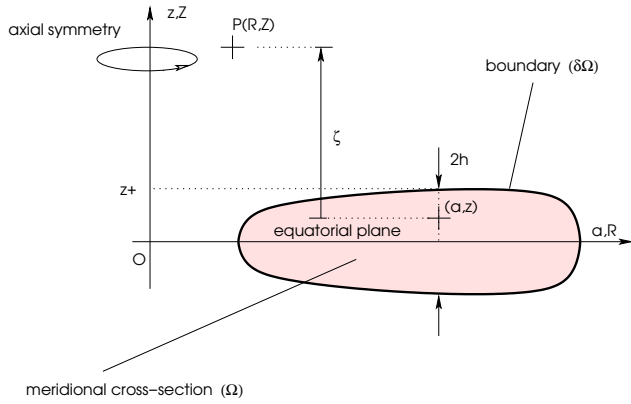


Figure 1. Typical configuration for the gravitating, axially symmetric body (finite size and mass, and local total thickness $2h$) and notations associated with the cylindrical coordinate system.

In a series of papers (Huré & Pierens 2005; Huré & Hersant 2007; Huré et al. 2007, 2008; Huré & Hersant 2011), we have mainly investigated flat, axially symmetric discs where the surface density is a power-law of the equatorial radius, with a special attention to edge effects. In this paper, we consider, as in Pierens & Huré (2005), systems with finite thickness, and present a new decomposition of the gravitational Green kernel which permits to express the potential as a sum of two regular integrals. These two integrals have interesting properties and their expression can give rise to very accurate approximations in the limit of geometrically thin discs, i.e. when the vertical thickness h of the disc is small enough.

This paper is organized as follows. In Section 2, we recall the general expression for the potential valid under axial symmetry and define the associated “mean Green function” to be calculated. In Section 3, we demonstrate that this mean function — an improper integral — can be rewritten as the sum of a regular, line integral over the boundary of the system and of an analytical function, also regular. This enables to rewrite the expression for the potential in a different, more tractable form which contains a surface integral and a line integral. This is the aim of Section 4. In Section 5, we briefly verify that the new expression for the potential automatically fulfills the right conditions at infinity. The question of the reduction of the remaining surface integral is addressed in Section 6. In Section 7, we build an approximation for the mean Green function from a first-order Taylor expansion (systems with small aspect ratios). We check the accuracy of the approximation and associated potential in Section 8 through a typical toroidal configuration. In Section 9, we show that stratification effects remain weak inside and outside the source, as soon as the total surface density is conserved. The last Section is devoted to a conclusion. A few useful formulae and demonstrations are found in Appendix.

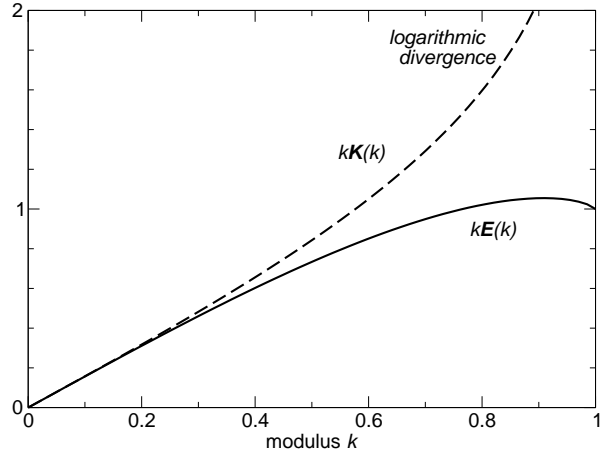


Figure 2. Variation of $k\mathbf{K}(k)$ and $k\mathbf{E}(k)$ with the modulus k . The first function logarithmically diverges as $k \rightarrow 1$, while the second function is bounded (and takes its maximal value for $k \approx 0.91$).

2 THE GRAVITATIONAL POTENTIAL UNDER AXIAL SYMMETRY. THEORETICAL GROUNDS

We consider an axially symmetric disc defined by its meridional cross-section (Ω) and mass density ρ , as depicted in Fig. 1. The gravitational potential ψ of this body is given, in cylindrical coordinates (R, Z) , by the surface integral (e.g. Durand 1953):

$$\psi(R, Z) = -2G \iint_{(\Omega)} \sqrt{\frac{a}{R}} \rho(a, z) k\mathbf{K}(k) da dz, \quad (1)$$

where (a, z) refers to points inside (Ω) belonging to the source, $\mathbf{K}(k)$ is the complete elliptical integral of the first kind (see the Appendix A for its definition),

$$k = \frac{2\sqrt{aR}}{\sqrt{(a+R)^2 + \zeta^2}} \in [0, 1], \quad (2)$$

is the modulus, and $\zeta = Z - z$ is the altitude difference. The divergence of the term $1/|\vec{r} - \vec{r}'|$ when $\vec{r} \rightarrow \vec{r}'$ initially present in Newton’s law still exists here through the function $\mathbf{K}(k)$ which logarithmically diverges¹ as $k \rightarrow 1$ (corresponding to $a = R$ and $z = Z$). This singularity is clearly visible in Fig. 2 where we have plotted the function $k\mathbf{K}(k)$ versus k . Although $\mathbf{K}(k) \rightarrow \infty$ as $k \rightarrow 1$, the integral of the potential is finite (Kellogg 1929; Durand 1953). Outside the material domain (Ω) , Eq.(1) can be easily evaluated numerically as the modulus k is always less than unity. But difficulties begin as one approaches the boundary $(\partial\Omega)$. Inside the source, the direct computation of the integral by standard numerical techniques cannot lead to accurate potential values due to the improper integral (at the location where k reaches unity). The separate treatment of the logarithmic divergence (see note 1) gives good results in terms

¹ Precisely, we have (Gradshteyn & Ryzhik 1965):

$$\mathbf{K}(k) \underset{k \rightarrow 1}{\sim} \ln 4 - \ln \sqrt{1 - k^2} \quad (3)$$

of precision (Ansorg et al. 2003; Huré 2005; Bannikova et al. 2011), but this approach is not very tractable. For these reasons, the Green function is generally replaced by its series expansion in Legendre polynomials. This effectively removes the divergence but generates new problems in practice (low convergence rate of the alternate series, truncations, etc.; see e.g. Clement 1974; Hachisu 1986).

The way to perform the double integral in Eq.(1) depends more or less on the mass density distribution and body’s shape via the equation for its boundary ($\partial\Omega$). If this equation can be defined by two bijections of the form $z_{\pm}(a)$ (i.e. z_+ above the equatorial plane and z_- below), then we can perform the integral over z first, followed by the integral over a . This is the most natural approach to treat geometrically thin discs and rings (e.g. Shakura & Sunyaev 1973; Pringle 1981), and this is the case we will consider in the following. The body is then regarded as a collection of *infinitely thin cylinders*. Assuming that the mass density does not depend upon z but only varies with the radius a , Eq.(1) can be written in the form:

$$\psi(R, Z) = -G \int_a \mathcal{G}(R, Z; a, z_{\pm}(a)) \Sigma(a) da, \quad (4)$$

where

$$\Sigma(a) = \int_z \rho(a) dz \quad (5)$$

is the total surface density in the disc, and

$$\mathcal{G} \equiv \int_z 2\sqrt{\frac{a}{R}} k \mathbf{K}(k) dz / \int_z dz \quad (6)$$

plays the role of a “mean Green function”. Actually, $\mathbf{K}(k)$ rises around $a = R$ and $\zeta = 0$, while it has small amplitude elsewhere ($\mathbf{K}(k) \rightarrow \frac{\pi}{2}$ for small k). Due to the integration process, \mathcal{G} is expected to be a regular function, peaking around $a = R$ (see below). It seems that *this integral is not known in closed-form*, but only through an alternate series whose convergence rate is unfortunately low (Durand 1953)².

For certain configurations where $z_{\pm}(a)$ is not bijective, it may be more convenient to integrate over a first, and then over z . This procedure is equivalent to considering the body as infinitely flat discs piled up along the z -direction³. Finally, it is worth mentioning that the double integral over the meridional cross-section can be converted, under certain conditions, into a line integral over the boundary ($\partial\Omega$) through the curl theorem which writes:

$$\int_{(\Omega)} (\partial_a N - \partial_z M) da dz = \int_{(\partial\Omega)} (M da + N dz), \quad (7)$$

under axial symmetry. Here, this requires the existence of two cylindrical functions $M(a, z)$ and $N(a, z)$ such that:

$$-2\sqrt{\frac{a}{R}} \rho k \mathbf{K}(k) = \partial_a N - \partial_z M. \quad (8)$$

² Actually, in contrast with the two components of the gravitational acceleration due to a *thin cylinder*, the potential is apparently available only through the series (Durand 1953).

³ The formula for homogeneous, infinitely thin disc is given in Durand (1953) (see also Lass & Blitzer 1983; Fukushima 2010; Tresaco et al. 2011).

This is not guaranteed in the general case where density gradients are present. However, Ansorg et al. (2003) have solved this question in the fully homogeneous case, i.e. when ρ is a constant.

3 BYPASSING THE KERNEL SINGULARITY: THE CASE OF VERTICALLY HOMOGENEOUS SYSTEMS

The absence of any closed-form for \mathcal{G} is problematic for most theoretical and numerical applications. We can however rewrite this mean Green kernel in another, more convenient form, as follows. By using various relationships involving the complete elliptic integrals of the first, second and third kind (\mathbf{K} , \mathbf{E} and $\mathbf{\Pi}$ respectively; see the Appendix A for their definition), we have established by direct calculus the following two formulae, valid for any integers n and p :

$$\partial_{\zeta} \zeta^n k^p \mathbf{K}(k) = \frac{\zeta^{n-1} k^p}{m^2} \left\{ [(n-p+1)m^2 + (p-1)k^2] \mathbf{K}(k) + (k^2 - m^2) \frac{\mathbf{E}(k)}{k'^2} \right\}, \quad (9)$$

and

$$\partial_{\zeta} \zeta^n k^p \mathbf{\Pi}(m, k) = \frac{\zeta^{n-1} k^p}{m^2} \left\{ [(n-p)m^2 + (p-1)k^2] \mathbf{\Pi}(m, k) + k^2 \frac{\mathbf{E}(k)}{k'^2} \right\}. \quad (10)$$

where

$$m = \frac{2\sqrt{aR}}{a+R}, \quad (11)$$

is the characteristic or parameter of $\mathbf{\Pi}$, and

$$k' = \sqrt{1-k^2} \quad (12)$$

is the modulus complementary of k . Note that $m \rightarrow k$ as $\zeta \rightarrow 0$ and $0 \leq k \leq m \leq 1$. If we now combine together Eqs.(9) and (10), with weights 1 and $m'^2 = 1 - m^2$ respectively, we get the general formula:

$$\begin{aligned} \partial_{\zeta} \zeta^n k^p \mathbf{K}(k) - m'^2 \partial_{\zeta} \zeta^n k^p \mathbf{\Pi}(m, k) &= \frac{\zeta^{n-1} k^p}{m^2} \\ &\times \left\{ [(n-p+1)m^2 + (p-1)k^2] \mathbf{K}(k) \right. \\ &\quad \left. - m'^2 [(n-p)m^2 + (p-1)k^2] \mathbf{\Pi}(m, k) - m^2 \mathbf{E}(k) \right\}. \end{aligned} \quad (13)$$

The remarkable point is that, for $p = 1$ and $n = p$, the complete elliptic of the third kind disappears in the right-hand-side, and we get:

$$\partial_{\zeta} \zeta k \mathbf{K}(k) - m'^2 \partial_{\zeta} \zeta k \mathbf{\Pi}(k) = k \mathbf{K}(k) - k \mathbf{E}(k). \quad (14)$$

As m does not depend on the relative altitude ζ , we can write this relation as:

$$\partial_{\zeta} \left\{ \zeta \left[k \mathbf{K}(k) - m'^2 k \mathbf{\Pi}(k) \right] \right\} = k \mathbf{K}(k) - k \mathbf{E}(k). \quad (15)$$

Finally, given $d\zeta = -dz$, it follows that⁴:

$$\int k \mathbf{K}(k) dz = \int k \mathbf{E}(k) dz - \zeta \mathbf{H}(m, k) \quad (16)$$

⁴ Huré & Dieckmann (2012) make another use of this relationship.

where \mathbf{H} is defined by

$$\mathbf{H}(m, k) = k \left[\mathbf{K}(k) - m'^2 \mathbf{\Pi}(m, k) \right]. \quad (17)$$

We recognize in the left-hand-side of Eq.(16) the expression coming into the definition of our “mean Green function”, in Eq.(6). This new form is very interesting. Actually, the first term in the right-hand-side of Eq.(16) is fully regular since $\mathbf{E}(k) \in [\frac{\pi}{2}, 1]$. The function $k\mathbf{E}(k)$ is displayed versus k in Fig. 2 and it is to be compared with the initial kernel $k\mathbf{K}(k)$. The second term is also fully regular and bounded. The divergence of $\mathbf{H}(m, k)$ when k and m both approach unity is cancelled out by the presence of the two vanishing factors m'^2 and ζ . The \mathbf{H} -function is plotted versus m and k/m in Appendix B. We conclude that Eq.(16) has a three satisfactory properties: i) it no longer contains any singular integrand, ii) it ensures that the effect of initial singularity is automatically accounted for, and iii) it fully saves the Newtonian properties of the potential and associated forces.

4 A GENERAL EXPRESSION FOR THE NEWTONIAN POTENTIAL OF VERTICALLY HOMOGENEOUS BODIES

By inserting Eq.(16) in Eq.(6), we find that the mean Green function associated with vertically homogeneous systems writes:

$$\mathcal{G}(R, Z; a, z_{\pm}) = \sqrt{\frac{a}{R}} \frac{1}{h} \left[\int_{z_-}^{z_+} k\mathbf{E}(k) dz - \zeta_+ \mathbf{H}(m, k_+) + \zeta_- \mathbf{H}(m, k_-) \right], \quad (18)$$

where, from Eq.(2):

$$k_{\pm} = \frac{2\sqrt{aR}}{\sqrt{(a+R)^2 + \zeta_{\pm}^2}}, \quad (19)$$

and $\zeta_{\pm} = Z - z_{\pm}$ is eventually a function of a (sign + being associated with the top boundary, and sign - is for the bottom). Since $k_{\pm} = 1$ only when $\zeta_{\pm} = 0$, the $\zeta\mathbf{H}$ terms in Eq.(18) are always finite. It means that the integration of the mean Green function over the radius a — see Eq.(4) — can be performed numerically without much difficulty as soon as $z_{\pm}(a)$ is known. In this integration process, some care must be taken though. Actually, when regarded as a function of a , $\mathbf{H}(m, k)$ is not derivable at $R = a$. The jump in the derivative can, however, be determined (see Sect. 8 and Appendix C). Depending on (R, Z) , this jump is:

- 0, outside the body,
- π , on the boundary ($\partial\Omega$),
- 2π , inside the domain (Ω).

As a result, \mathcal{G} is peaked at $a = R$, and the maximum value \mathcal{G}_{\max} is:

$$\mathcal{G}_{\max} \equiv \mathcal{G}(R, Z; R, z_{\pm}) \quad (20)$$

$$= \frac{1}{h(R)} \left[\int_{z_-}^{z_+} k\mathbf{E}(k) dz - \zeta_+ k_+ \mathbf{K}(k_+) + \zeta_- k_- \mathbf{K}(k_-) \right].$$

Note that, for a flat body, $z_{\pm} = 0$ and so one recovers

the well-known expression:

$$\mathcal{G}(R, Z; a, 0) = 2\sqrt{\frac{a}{R}} k\mathbf{K}(k). \quad (21)$$

The general expression for the gravitational potential is then found from Eqs. (4) and (18), namely:

$$\psi(R, Z) = -G \int_a \Sigma(a) \frac{1}{h} \sqrt{\frac{a}{R}} da \int_{z_-}^{z_+} k\mathbf{E}(k) dz \quad (22)$$

$$+ G \int_a \Sigma(a) \sqrt{\frac{a}{R}} \frac{1}{h} [\zeta_+ \mathbf{H}(m, k_+) - \zeta_- \mathbf{H}(m, k_-)] da.$$

We recall that this expression is exact and valid for any point (R, Z) of space, for any surface density profile $\Sigma(a)$ (no vertical density gradients), and semi-thickness $h(a)$. It contains a surface integral over (Ω) and a line integral over ($\partial\Omega$) through $z_{\pm}(a)$.

If the body is symmetric with respect to the equatorial plane, we have $z_+ = -z_- = h$. Unfortunately, Eq.(18) does not simplify more since k_+ and k_- remain different, except for $Z = 0$. This case corresponds to the potential at the midplane. With $\zeta_+ = -\zeta_- = -h$, the midplane mean Green function writes:

$$\mathcal{G}(R, 0; a, h) = 2\sqrt{\frac{a}{R}} \left[\frac{1}{h} \int_0^h k\mathbf{E}(k) dz + \mathbf{H}(m, k_{\pm}) \right] \quad (23)$$

and

$$\mathcal{G}_{\max} = 2 \left[\frac{1}{h(R)} \int_0^h k\mathbf{E}(k) dz + k_{\pm} \mathbf{K}(k_{\pm}) \right]. \quad (24)$$

5 LONG-RANGE PROPERTIES

We can check that the long-range properties of the potential defined by Eq.(22) are correct. Actually, far enough from the system, the potential is expected to tend towards the potential due to a central condensation, or

$$\lim_{r \rightarrow \infty} r\psi = -GM, \quad (25)$$

where $r = \sqrt{R^2 + Z^2}$ is the spherical radius, and

$$M = 2\pi \int_a a\Sigma(a) da \quad (26)$$

is the total mass. We see that $k \approx 2\sqrt{aR}/r \rightarrow 0$ as $r \rightarrow \infty$, and then $\mathbf{E}(k) \rightarrow \pi/2$. It means that the long-range behavior is ensured by the first term in the right-hand-side of Eq.(22) containing the complete elliptic integral of the second kind \mathbf{E} , whereas the contribution from the \mathbf{H} -function is a higher-order correction (see Appendix D for a more detailed analysis).

6 FULL REDUCTION TO A ONE-DIMENSIONAL INTEGRAL ?

The important question we have tried to clarify concerns the possibility to convert the remaining double integral in the right-hand-side of Eq.(22) into a line integral (by performing the integral over z or ζ). Actually, the existence of a compact expression for

$$\int k\mathbf{E}(k)d\zeta \quad (27)$$

would be helpful, since the potential ψ of a tri-dimensional, vertically homogeneous and axially symmetric system would be given by a one-dimensional integral. This is the reason why we have explored different paths, but unsuccessfully. We have for instance re-written $k\mathbf{E}(k)$ in the form of an infinite series over k , or re-considered $\mathbf{E}(k)$ as an integral over ϕ , followed by term-by-term integration as done in Cvijović & Klinowski (1994). However, none of these two approaches leads, apparently, to a closed-form in the general case. Equation (27) can also be converted into various equivalent forms, like:

$$\int k\mathbf{E}(k)d\zeta = \pm \frac{4aR}{a+R} \int \frac{\mathbf{E}(k)dk}{k\sqrt{m^2-k^2}}, \quad (28)$$

where $\pm = |\zeta|/\zeta$. This integral over k is known only for $m = 1$. In particular, the indefinite form has been derived by Dieckmann (2011; private communication⁵), but it involves hypergeometric series which are not easy to manipulate. The definite form⁶ is known only when the integral bounds are 0 and 1 (Cvijović & Klinowski 1994; Cvijovic & Klinowski 1999; Prudnikov et al. 1988) which corresponds to ζ in the range $]\pm\infty, 0]$. This is a very special situation: a and R are obviously different in general, and so the case $m = 1$ is too restrictive. Finally, following Ansorg et al. (2003), we have also searched for a two-component vector (M', N') whose curl would yield the function $\sqrt{\frac{a}{R}}k\mathbf{E}(k)$ (see Sect. 2), but we failed to find a simple and convincing answer. This question remains therefore open.

7 APPLICATION TO GEOMETRICALLY THIN DISCS AND RINGS: A USEFUL AND ACCURATE APPROXIMATION

The main assumption made up to now is the absence of vertical stratification for the mass density. It is true that, except

⁵ See <http://pi.physik.uni-bonn.de/~dieckman/>

⁶ The definite integral can take various equivalent form, like:

$$\begin{aligned} \int_{\infty}^{\zeta_+} k\mathbf{E}(k)d\zeta &= 2\sqrt{aR} \int_{\infty}^{u_+} \mathbf{E}(m \operatorname{sech}(u)) du \\ &= 2\sqrt{aR} \int_0^{v_+} \frac{\mathbf{E}(mv)dv}{vv'} \\ &= \frac{2\sqrt{aR}}{k_+} \int_0^1 \frac{\mathbf{E}(tk_+)dt}{t\sqrt{1-\frac{k_+^2}{m^2}t^2}} \end{aligned} \quad (29)$$

where

$$\zeta = (a+R) \sinh u, \quad (30)$$

$$v = \operatorname{sech}(u), \quad (31)$$

and

$$t = \frac{k}{k_+}, \quad (32)$$

which can unfortunately not be reduced more, because formulae linking complete elliptic integrals with different moduli, for instance $\mathbf{E}(\alpha x)$ and $\mathbf{E}(x)$ for any real $\alpha \in]0, 1]$, are missing (Landen and Gauss transformations are useless here).

for very academic (i.e. unrealistic) configurations, this may a priori not apply to astrophysical problems — however, as we show in Section 9, the sensitivity to stratification remains weak. Possible domains of interest concern certain polytropic fluids (e.g. Hachisu 1986; Ansorg et al. 2003), and geometrically thin discs and rings (Pringle 1981). For thin discs actually, radial gradients are often neglected over vertical gradients (Pringle 1981), at least far from edges. In this context, a vertically averaged structure with a uniform density along the z -axis is commonly assumed (Shakura & Sunyaev 1973; Collin-Souffrin & Dumont 1990; Dubrulle 1992). Their total thickness $2h(a) \equiv z_+ - z_-$ is everywhere small compared to the radius a , which enables many developments. Regarding the present problem, it means that k_+ and k_- are always close to each other. We can, in this case, produce an approximation for the mean Green function (and thus for the potential) by estimating Eq.(27). There are various ways to address the problem. In order to get an approximation valid in the whole physical space (and not only in the disc vicinity as often considered), it is appropriate to work with the mean modulus \tilde{k} defined by:

$$\tilde{k} = \frac{k_+ + k_-}{2}. \quad (33)$$

In particular, \tilde{k} never reaches unity⁷, preventing any eventual divergence of the elliptic integrals. If we now perform a Taylor expansion of $k\mathbf{E}(k)$ around \tilde{k} , we obtain, at first order:

$$k\mathbf{E}(k) \approx \tilde{k}\mathbf{E}(\tilde{k}) + \left. \frac{d}{dk}k\mathbf{E}(k) \right|_{\tilde{k}} (k - \tilde{k}), \quad (34)$$

and then (see the appendix A for the derivative):

$$k\mathbf{E}(k) \approx \tilde{k}\mathbf{E}(\tilde{k}) + [2\mathbf{E}(\tilde{k}) - \mathbf{K}(\tilde{k})] (k - \tilde{k}), \quad (35)$$

which is always bounded since $\tilde{k} < 1$. The truncation produces an error of the order of $(k - \tilde{k})^2$. We can now estimate the integral of $k\mathbf{E}(k)$ with respect to z or ζ . After re-arranging terms, we can write this integral as:

$$\int_{\zeta} k\mathbf{E}(k)d\zeta \approx \mathbf{T}_1(\tilde{k})\zeta + \mathbf{T}_2(\tilde{k}) \int_{\zeta} kd\zeta \quad (36)$$

where we have defined:

$$\mathbf{T}_1(k) = k [\mathbf{K}(k) - \mathbf{E}(k)] \equiv k^3\mathbf{D}(k), \quad (37)$$

and

$$\mathbf{T}_2(k) = 2\mathbf{E}(k) - \mathbf{K}(k) \equiv \mathbf{E}(k) - k^2\mathbf{D}(k). \quad (38)$$

where $\mathbf{D}(k)$ is another common complete elliptic integral (see the Appendix A). These two functions are plotted versus k in Fig. 3. Note that \mathbf{T}_1 and \mathbf{T}_2 logarithmically diverge as $k \rightarrow 1$. This is not a problem since these functions are always invoked with a modulus less than one. Besides,

⁷ This is true except when $z_+ = z_-$ and $Z = 0$. This case is met when the potential is requested in the equatorial plane, at radii where the thickness is zero. This is precisely the case of “edges” where the mass density ρ is also expected to vanish. So, we can conclude that $\tilde{k} < 1$ for realistic configurations.

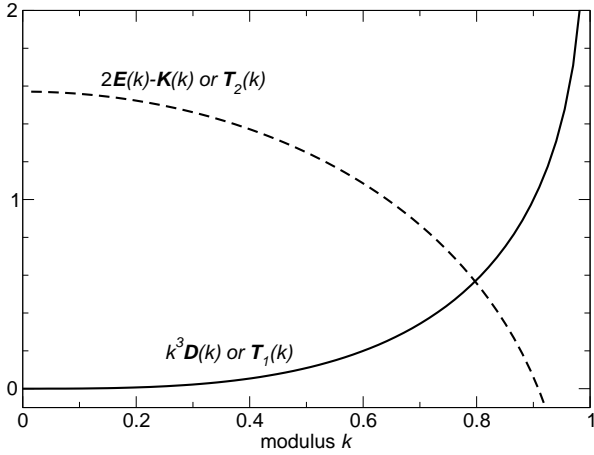


Figure 3. Variation of $\mathbf{T}_1(k)$ and $\mathbf{T}_2(k)$ with the modulus k . These two functions logarithmically diverge as $k \rightarrow 1$.

the integration of k with respect to ζ is easily found analytically:

$$\int_{\zeta} k d\zeta = \int_{\zeta} \frac{2\sqrt{aR}}{\sqrt{(a+R)^2 + \zeta^2}} d\zeta \quad (39)$$

$$= 2\sqrt{aR} \operatorname{argsh} \left(\frac{\zeta}{a+R} \right).$$

By replacing in Eq.(18) the vertical integral by Eq.(36), its approximation, we find the “approximate mean Green function”:

$$\mathcal{G}_{\text{app.}}(R, Z; a, z_{\pm}) = 2\sqrt{\frac{a}{R}} \left\{ \mathbf{T}_1(\tilde{k}) \right. \quad (40)$$

$$\left. - \mathbf{T}_2(\tilde{k}) \frac{\sqrt{aR}}{h} \left[\operatorname{argsh} \left(\frac{\zeta_+}{a+R} \right) - \operatorname{argsh} \left(\frac{\zeta_-}{a+R} \right) \right] \right.$$

$$\left. - \frac{\zeta_+}{2h} \mathbf{H}(m, k_+) + \frac{\zeta_-}{2h} \mathbf{H}(m, k_-) \right\}.$$

where \tilde{k} is given by Eq.(33). The error is expected to be of the order of $\int_z (k - \tilde{k})^2 dz$. The approximation for the potential is given by Eq.(4) where \mathcal{G} is to just be replaced by $\mathcal{G}_{\text{app.}}$, or:

$$\psi(R, Z) \approx -G \int_a \Sigma(a) \mathcal{G}_{\text{app.}}(R, Z; a, z_{\pm}) da. \quad (41)$$

As this approximation works in the whole physical space (no hypothesis has been made upon R and Z), it can be used not only to model the internal structure of self-gravitating discs and rings, but also for dynamical studies where the system is basically a source of gravity acting on external, moving particles (e.g. Šubr & Karas 2005; Tresaco et al. 2011). Equation (41) is also attractive from a numerical point of view as it involves a one dimensional integral, with finite integrand.

The long-range properties of the potential are automatically conserved here as, in deriving this approximation, we have made no hypothesis about the relative distance to the system. When $r \rightarrow \infty$, we have $\tilde{k} \sim 2\sqrt{aR}/r \rightarrow 0$, and so $2\mathbf{T}_2(\tilde{k}) \sim \pi$ while $4\mathbf{T}_1(\tilde{k}) \sim \pi\tilde{k}^2$ (the \mathbf{H} -function brings a similar, second-order correction; see the Appendix E). The

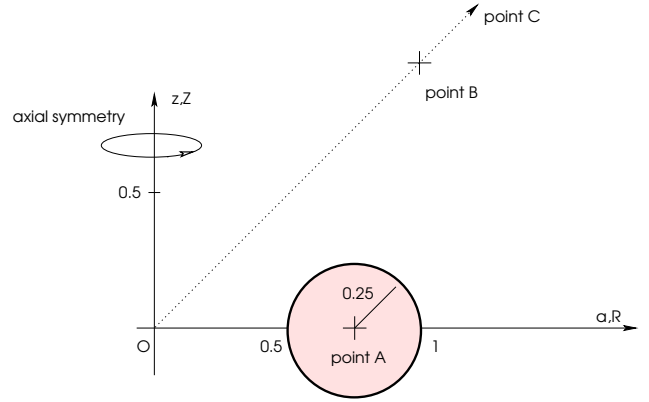


Figure 4. A test-torus with circular cross-section, and edges at $\frac{1}{2}$ and 1 (see Fig. 5 for the mean Green function at points A, B and C).

main contribution in the potential then comes from $\mathbf{T}_2(\tilde{k})$:

$$\psi(R, Z) \approx -G \int \Sigma(a) \sqrt{\frac{a}{R}} (-\pi\tilde{k})(-2h) da \quad (42)$$

$$\sim -4\pi G \frac{1}{r} \int \Sigma(a) a da$$

$$\sim -\frac{GM}{r}.$$

8 A NUMERICAL EXAMPLE

To check the quality of the approximate potential, it is not necessary to compare Eq.(4) or Eq.(22) together with Eq.(41). It is sufficient to compare the two Green functions, i.e. \mathcal{G} and its approximation $\mathcal{G}_{\text{app.}}$. Since the approximation made does not involve the \mathbf{H} -function (it is the same for both expressions), we can simply consider the two members of Eq.(36). To perform this comparison, we have considered a homogeneous torus with circular cross-section, inner edge $a_{\text{in}} = \frac{1}{2}$ and outer edge $a_{\text{out}} = 1$ as depicted in Fig. 4. A similar test-torus has been considered in Bannikova et al. (2011). Also, in order to show how the mean Green function behaves (\mathcal{G} also depends on R and Z), we have selected three points where the potential could be requested:

- point A ($\frac{3}{4}, 0$) inside the torus (at the center),
- point B(1, 1), outside it,
- point C (10, 10), relatively “far away” from the system.

Figure 5 displays the mean Green function \mathcal{G} versus the radius a at points A, B and C. As expected (see Section 2), the function is the largest when (R, Z) stands inside the disc (the case of point A) and peaks at $a = R$, with a jump in the derivative (due to the \mathbf{H} -function; see the Appendix C). At point A, we have $k_{\pm} \approx 0.9864$, $\mathbf{K}(k_{\pm}) \approx 3.21$ and $\int k \mathbf{E}(k) dz \approx 0.450$ (see i.e. Eq.(39)), and so $\mathcal{G}_{\text{max.}} \approx 8.32$ from Eq.(20). Outside the system (points B and C), \mathcal{G} has a much lower amplitude, but still exhibits a minimum. The relative difference between \mathcal{G} and its approximation $\mathcal{G}_{\text{app.}}$ is shown in Fig. 6 for points A and B, and in Fig. 7 for point C. According to the Taylor expansion (see Sect. 7), the absolute error is given by $\int_z (k - \tilde{k})^2 dz$. This term is easy to calculate. Inside the system and in its close neighbourhood,

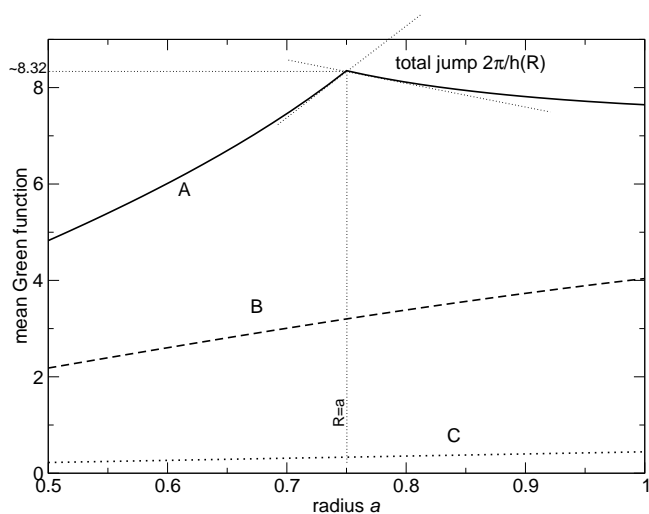


Figure 5. Variation of the mean Green function \mathcal{G} with the radius a at points A, B and C for the test-torus considered in Sect. 8 (see also Fig. 4). Inside the system, the radial derivative of the \mathcal{G} -function undergoes a jump at $R = a$ where the function peaks (the case of point A), due to the **H**-function (see text).

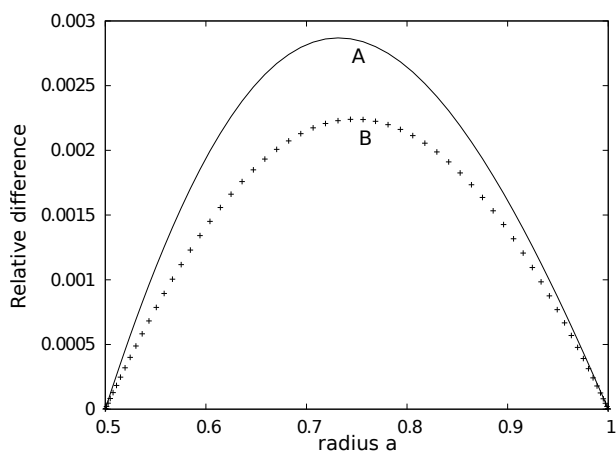


Figure 6. Relative difference between the mean Green function \mathcal{G} and its approximation \mathcal{G}_{app} , versus a at points A (plain line) and B (crosses) for the test-torus shown in Fig. 4.

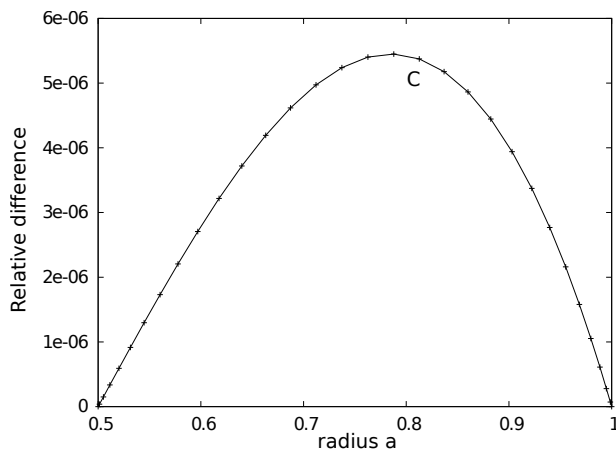


Figure 7. Same legend as Fig. 6 but for point C.

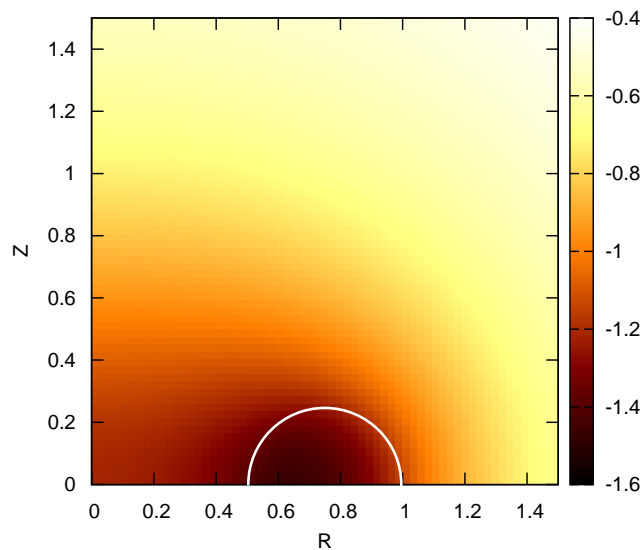


Figure 8. Potential of the homogeneous torus computed from Eq.(22) at the nodes of a regular (R, Z) -grid (64×64 nodes; R and $Z \in [0, 1.5]$). The torus has circular cross-section (shown in white), a diameter $\frac{1}{2}$, and outer edge $a_{\text{out}} = 1$.

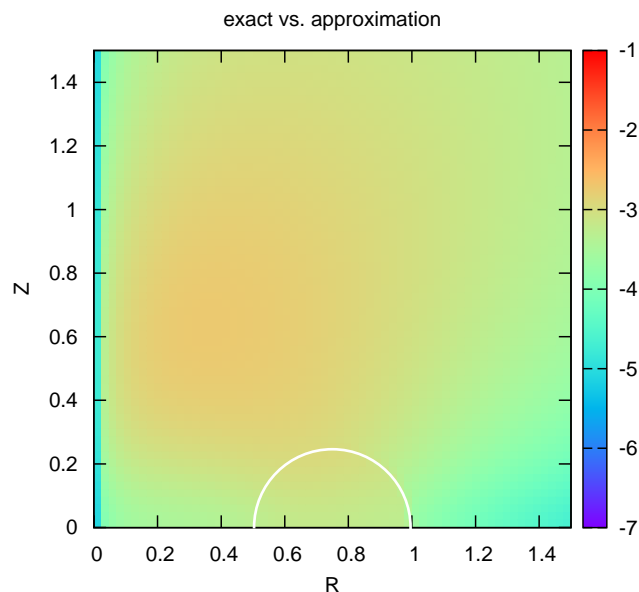


Figure 9. Relative error (decimal log. scale) in potential values when using the approximation Eq. (41) rather than Eq.(22). The conditions are the same as for Fig. 8.

we find that the error is $\sim h^4/(a+R)^4$. This is a relatively small error for geometrically thin discs (most quantities have a precision of $\sim (h/a)^2$ in general). In the present example where h reaches 0.25, the absolute error is expected to be $\sim 10^{-3}$ which is compatible with what we observe for points A and B. The error in potential values (the area under the curves) is therefore of the order of $\sim h^4/(a+R)^4 \times \Delta a$ here, where Δa is the radial extension of the system. This is therefore $\sim 3 \times 10^{-4}$ for point A and for point B, and $\sim 3 \times 10^{-6}$ for point C (see the error map below).

We have computed the potential map in the vicinity of the torus from Eq. (4), using the exact mean Green function

\mathcal{G} . The result is shown in Fig. 8. We have also determined the approximate potential from Eq.(41), that is, using the approximate Green function $\mathcal{G}_{\text{app.}}$. The relative error (log. scale) between the two potential maps is shown in Fig. 9. We conclude that we have, through the approximation, still a very precise estimate of $\int k\mathbf{E}(k)d\zeta$ inside as well as outside the system. This is not that surprising since $\mathbf{E}(k)$ is a regular function.

It is worth noting that the actual test-torus, with $\frac{h}{a} \approx 0.33$, does not correspond to what is usually called a “geometrical thin” system. But as the error is of the order $\mathcal{O}(h^4/a^4)$, Eq.(41) remains valid for relatively thick systems, including thick discs and tori.

9 INFLUENCE OF VERTICAL STRATIFICATION

As realistic systems are expected to have density gradients in the three directions, it is important to check the sensitivity of the results obtained so far to the $\rho(z)$ profile. This can easily be done, still assuming axial symmetry, by introducing the *inhomogeneous analog* of Eq.(6) defined by:

$$\mathcal{G}^{\text{in.}} \equiv \int_z 2\sqrt{\frac{a}{R}}\rho(z)k\mathbf{K}(k)dz \Big/ \int_z \rho(z)dz. \quad (43)$$

For geometrically thin disc models, the mass density often consists in a power-law of the radius combined with a Gaussian profile in the direction perpendicular to the midplane, which is a direct consequence of a locally isothermal gas in hydrostatic equilibrium (Pringle 1981; Müller et al. 2012). As long as we can decouple the radial and vertical density structures, an interesting profile is therefore the following

$$\rho(z) = 2\rho_0\sqrt{\frac{2}{\pi}}\exp\left(-\frac{2z^2}{h^2}\right), \quad (44)$$

where $z \in]-\infty, \infty[$ and ρ_0 is a constant, possibly a function of the radius. We have also considered the parabolic profile, namely

$$\rho(z) = \frac{3}{2}\rho_0\left[1 - \left(\frac{z}{h}\right)^2\right], \quad (45)$$

where $z \in [-h, h]$. This profile is very similar to the Gaussian law, matter being however confined into a finite domain. For these two inhomogeneous profiles, the surface density is $2\rho_0h$, as for the vertically homogeneous case, while central values are different (1.5 and ≈ 1.59 and 1, respectively). Figure 10 shows $\mathcal{G}^{\text{in.}}(a)$ computed from Eq.(43) for the two inhomogeneous profiles for the torus considered in the previous section, at the interior point A. We see that the mean Green functions are very similar in shape, still peaking at $a = R$. The maximum is higher for the parabolic case and even higher for the Gaussian case (10% and 11% respectively with respect to the canonical case), due to larger and larger central values⁸. The difference on potential values (the area

⁸ More generally, for a vertical profile of the form:

$$\rho(z) = A + B\left(\frac{z}{h}\right)^2, \quad (46)$$

we can find a good approximation for $\mathcal{G}_{\text{max.}}$ by using the right expansion for $\mathbf{K}(k)$ (see note 1) followed by integrations terms by

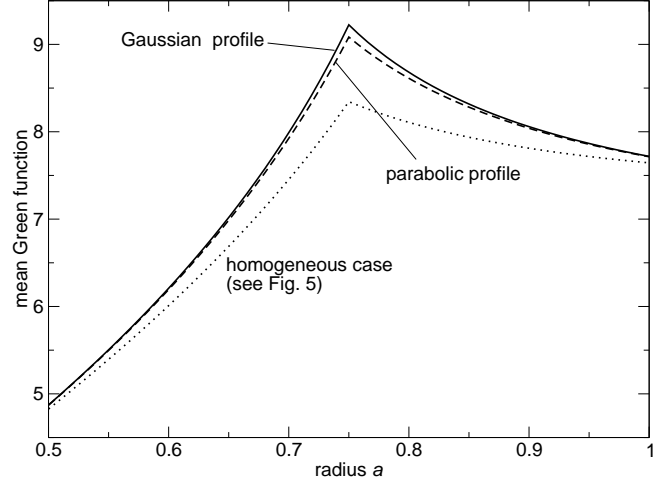


Figure 10. Variation of the mean Green function with the radius a at point A for the test-torus considered in Section 8 (see also Fig. 4) for three different profiles $\rho(z)$: the homogeneous case (see Fig. 5), the parabolic profile and the Gaussian profile.

under the curves) is however not that large, of the order of 5% (we have $\Psi_A \approx -1.504$ and -1.513 respectively, compared to -1.436 in the homogeneous case). The deviation is in excess, as expected: in general, the more concentrated the mass distribution, the deeper the potential well. We have performed the same comparison at points B and C which stand outside the torus. We have noticed that as we move away from the distribution, the relative difference between profiles gets smaller and smaller. Again, this is not really a surprise since at large distance, the potential tends to that of a point mass and the details of the distribution are no longer perceptible. Figure 11 shows the relative difference between the potential generated by a Gaussian profile and the homogeneous case. It turns out that the potential inside as well as outside the body is mainly sensitive to the surface density, which is therefore the critical parameter.

10 CONCLUSION

In this article, we have proposed an alternative definition of the potential of axially symmetrical bodies which avoids a singular kernel. This is based on the effective integration of the genuine kernel along the vertical direction. This naturally leaves a regularized kernel, called “mean Green function”, which peaks at the location of the initial logarithmic singularity but remains of finite amplitude. This is yet another proof that the local contribution of matter located at $\vec{r}' \approx \vec{r}$ is very important and may dominate the total contribution. This new but equivalent form is therefore attractive because the corresponding gravitational potential is then accessible from two classical integrals: the one over the body’s

terms. We then get:

$$\mathcal{G}_{\text{max.}} \approx 2\Sigma \ln \frac{8R}{h(R)} + 2Ah + \frac{2}{9}Bh \quad (47)$$

which leads to the correct values in the cases considered here, namely: ~ 8.32 for the homogeneous profile, ~ 9.02 for the parabolic profile and ~ 9.19 for the Gaussian profile.

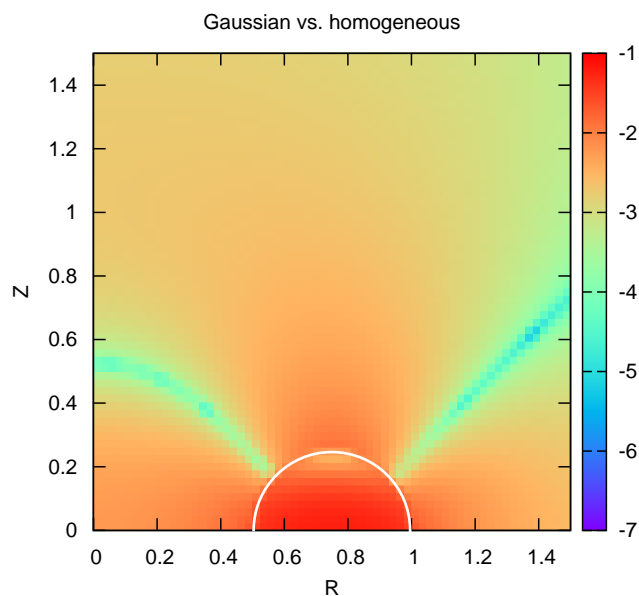


Figure 11. Relative error (decimal log. scale) in potential values between the Gaussian case and the homogeneous case (see text for more details). The conditions are the same as for Fig. 8.

meridional cross-section, and the other over the body’s equatorial radius. The total absence of diverging kernels means that there is no need for special meshing or specific numerical schemes. Also, the properties of Newton’s law are fully conserved with this approach.

Rigorously, our results are valid only for mass density profiles which are uniform along the z -axis, while there is no restriction about the (radial) surface density profile, thickness/shape and size of the system. This still makes the method relevant to various kinds of configurations, ranging from geometrically thin discs and rings found in different contexts (Collin-Souffrin & Dumont 1990; Dubrulle 1992; Arnaboldi & Sparke 1994), to possibly long, cylindrical/filamentary structures as observed in the interstellar medium (Curry 2000; Hennebelle 2003). The fact that the asymptotic, long-range behavior of the potential is well reproduced means that our formula can also be used to generate quickly and simply grids of potential in which the motion of test-particles can be studied. Nevertheless, we have analyzed a few inhomogeneous situations, in particular the Gaussian profile. It turns out that the sensitivity to stratification is weak on potential values. The local surface density remains the decisive parameter.

We failed to convert the mean Green function into a line integral — see Eq.(27) and note 6 — as done in Ansorg et al. (2003) with the genuine kernel $k\mathbf{K}(k)$. This does not seem possible unless new closed-form relationships between complete elliptic integrals with homothetical moduli are derived. Also, we have expanded at first-order the mean Green function around vanishing aspect ratio h/a , enabling to perform this conversion. We have then obtained an approximation with very small error. Accuracy can be improved by considering next terms.

ACKNOWLEDGMENTS

It is a pleasure to thank M. Ansorg, A. Bachelot, A. Dieckmann, J. Klinowski for opinions on different aspects of theoretical calculus, and M.-P. Pomies. We wish to thank the referee who suggested to comment about the influence of vertical stratification, which has led to Section 9.

REFERENCES

- Ambastha A., Varma R. K., 1983, *ApJ*, 264, 413
 Ansorg M., Kleinwächter A., Meinel R., 2003, *MNRAS*, 339, 515
 Arnaboldi M., Sparke L. S., 1994, *AJ*, 107, 958
 Bannikova E. Y., Vakulik V. G., Shulga V. M., 2011, *MNRAS*, 411, 557
 Baruteau C., Masset F., 2008, *ApJ*, 678, 483
 Binney J., Tremaine S., 1987, *Galactic dynamics*. Princeton, NJ, Princeton University Press, 1987, 747 p.
 Bodo G., Curir A., 1992, *A&A*, 253, 318
 Clement M. J., 1974, *ApJ*, 194, 709
 Cohl H. S., Tohline J. E., 1999, *ApJ*, 527, 86
 Collin-Souffrin S., Dumont A. M., 1990, *A&A*, 229, 292
 Cox D. P., Gómez G. C., 2002, *ApJS*, 142, 261
 Curry C. L., 2000, *ApJ*, 541, 831
 Cvijović D., Klinowski J., 1994, *Royal Society of London Proceedings Series A*, 444, 525
 Cvijovic D., Klinowski J., 1999, *Journal of Computational and Applied Mathematics*, 106, 169
 Dubrulle B., 1992, *A&A*, 266, 592
 Durand E., 1953, *Electrostatique. Vol. I. Les distributions..* Ed. Masson
 Fromang S., Balbus S. A., De Villiers J.-P., 2004, *ApJ*, 616, 357
 Fukushima T., 2010, *Celestial Mechanics and Dynamical Astronomy*, 108, 339
 Gradshteyn I. S., Ryzhik I. M., 1965, *Table of integrals, series and products*. New York: Academic Press, 1965, 4th ed., edited by Geronimus, Yu.V. (4th ed.); Tseytlin, M.Yu. (4th ed.)
 Hachisu I., 1986, *ApJS*, 61, 479
 Hennebelle P., 2003, *A&A*, 397, 381
 Huré J., Hersant F., 2007, *A&A*, 467, 907
 Huré J.-M., 2005, *A&A*, 434, 1
 Huré J.-M., Dieckmann A., 2012, *A&A*, in press (ArXiv e-prints 1203.6822)
 Huré J.-M., Hersant F., 2011, *A&A*, 531, A36
 Huré J.-M., Hersant F., Carreau C., Busset J.-P., 2008, *A&A*, 490, 477
 Huré J.-M., Hersant F., Surville C., Nakai N., Jacq T., 2011, *A&A*, 530, A145
 Huré J.-M., Pelat D., Pierens A., 2007, *A&A*, 475, 401
 Huré J.-M., Pierens A., 2005, *ApJ*, 624, 289
 Kellogg O. D., 1929, *Foundations of Potential Theory*. New-York: Frederick Ungar Publishing Company
 Lass H., Blitzler L., 1983, *Celestial Mechanics*, 30, 225
 Mestel L., 1963, *MNRAS*, 126, 553
 Müller T. W. A., Kley W., Meru F., 2012, *ArXiv e-prints*
 Pierens A., Huré J.-M., 2005, *A&A*, 434, 17
 Pringle J. E., 1981, *ARA&A*, 19, 137
 Prudnikov A. P., Brychkov Y. A., Marichev O. I., Romer R. H., 1988, *American Journal of Physics*, 56, 957

- Schulz E., 2009, ApJ, 693, 1310
 Schulz E., 2011, ArXiv e-prints
 Shakura N. I., Sunyaev R. A., 1973, A&A, 24, 337
 Stone J. M., Norman M. L., 1992, ApJS, 80, 753
 Tresaco E., Elipe A., Riaguas A., 2011, Celestial Mechanics and Dynamical Astronomy, pp 95–+
 Šubr L., Karas V., 2005, in S. Hledík & Z. Stuchlík ed., RAGtime 6/7: Workshops on black holes and neutron stars A manifestation of the Kozai mechanism in the galactic nuclei. pp 281–293
 Vogt D., Letelier P. S., 2010, MNRAS, 408, 1649
 Vogt D., Letelier P. S., 2011, MNRAS, 411, 2371

APPENDIX A: DEFINITIONS

The complete elliptic integral of the first, second and third kinds are defined by (Gradshteyn & Ryzhik 1965):

$$\mathbf{K}(k) = \int_0^{\pi/2} \frac{1}{\sqrt{1 - k^2 \sin^2 \phi}} d\phi, \quad (\text{A1})$$

$$\mathbf{E}(k) = \int_0^{\pi/2} \sqrt{1 - k^2 \sin^2 \phi} d\phi, \quad (\text{A2})$$

and,

$$\mathbf{\Pi}(m, k) = \int_0^{\pi/2} \frac{d\phi}{(1 - m^2 \sin^2 \phi) \sqrt{1 - k^2 \sin^2 \phi}}, \quad (\text{A3})$$

respectively, where k is the modulus and m is the characteristic or parameter. In the present study, we have $0 \leq k \leq m \leq 1$, k is defined by Eq.(2), so that $m = k$ for $\zeta = 0$. The function $\mathbf{D}(k)$ is defined by:

$$k^2 \mathbf{D}(k) = \mathbf{K}(k) - \mathbf{E}(k). \quad (\text{A4})$$

The demonstration given in Section 3 is based upon the following partial derivatives with respect to the modulus k (Gradshteyn & Ryzhik 1965):

$$\partial_k \mathbf{K}(k) = \frac{1}{k} \left[\frac{\mathbf{E}(k)}{k'^2} - \mathbf{K} \right], \quad (\text{A5})$$

$$k \partial_k \mathbf{E}(k) = \mathbf{E}(k) - \mathbf{K}(k), \quad (\text{A6})$$

and (Durand 1953):

$$\partial_k \mathbf{\Pi}(m, k) = \frac{k}{m^2 - k^2} \left[\mathbf{\Pi}(m, k) - \frac{\mathbf{E}(k)}{k'^2} \right], \quad (\text{A7})$$

where $k' = \sqrt{1 - k^2}$ is the complementary modulus.

We also have

$$\frac{\zeta}{2\sqrt{aR}} = \pm \frac{\sqrt{m^2 - k^2}}{mk} \quad (\text{A8})$$

where sign + stands for $\zeta > 0$, and then

$$\zeta \partial_\zeta k = \frac{k}{m^2} (k^2 - m^2). \quad (\text{A9})$$

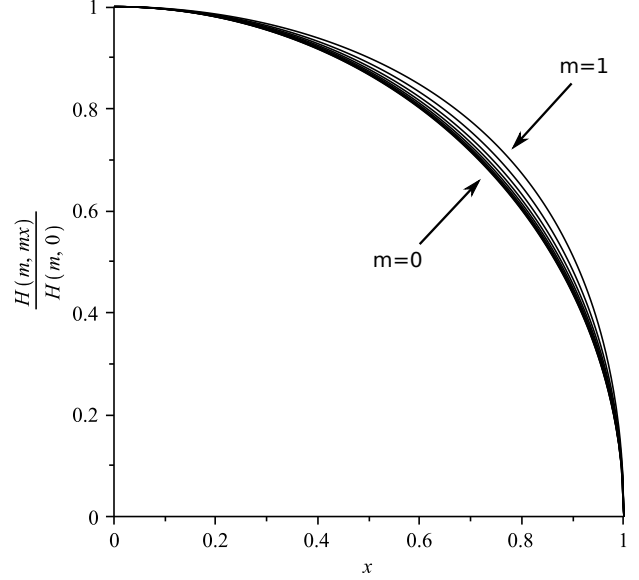


Figure B1. The function $\zeta \mathbf{H}(m, mx)$ normalized to its value at $x = 0$, versus x for different values of $m \in [0, 1]$.

APPENDIX B: THE FUNCTION H

The function $\mathbf{H}(m, k)$ defined in Section 3 can be rewritten in terms of the variable $x = \frac{k}{m} \in [0, 1]$, namely:

$$\mathbf{H}(m, mx) \equiv mx \left[\mathbf{K}(mx) - m'^2 \mathbf{\Pi}(m, mx) \right], \quad (\text{B1})$$

and so:

$$\frac{\mathbf{H}(m, mx)}{\mathbf{H}(m, 0)} = \frac{2}{\pi} x' \frac{\mathbf{K}(mx) - m'^2 \mathbf{\Pi}(m, mx)}{1 - m'}, \quad (\text{B2})$$

where

$$\mathbf{H}(m, 0) = \frac{\pi}{2} (1 - m'), \quad (\text{B3})$$

and $x' = \sqrt{1 - x^2}$. The ratio $\mathbf{H}(m, mx)/\mathbf{H}(m, 0)$ is plotted versus x and for different parameters m in Fig. B1. In a first approximation, we have from the figure $\mathbf{H}(m, k) \approx x' \mathbf{H}(m, 0)$, and so

$$\zeta \mathbf{H}(m, k) \approx \pm \frac{\pi}{2} (a + R) (1 - m') \frac{x'^2}{x}. \quad (\text{B4})$$

APPENDIX C: JUMP IN THE RADIAL DERIVATIVE OF THE FUNCTION $\mathbf{H}(M, K)$

When $a \rightarrow R$ (i.e. $m \rightarrow 1$) and for $\zeta \neq 0$, we have (Durand 1953):

$$m'^2 \mathbf{\Pi}(m, k) \underset{m \rightarrow 1}{\sim} \frac{\pi}{2} \frac{m'}{k'}. \quad (\text{C1})$$

As we have

$$\partial_a m' = \pm \frac{2R}{(a + R)^2}, \quad (\text{C2})$$

where sign + stands for $a > R$, we see that the jump in the derivative of $\mathbf{\Pi}$ at $a = R$ produces a jump in the derivative

of \mathbf{H} . This jump is calculated as follows:

$$\begin{aligned}
 \lim_{m \rightarrow 1} \partial_a m'^2 \mathbf{\Pi}(m, k) &= \partial_a \lim_{m \rightarrow 1} m'^2 \mathbf{\Pi}(m, k) \quad (\text{C3}) \\
 &= \partial_a \frac{\pi}{2} \frac{m'}{k'} \\
 &= \frac{\pi}{2} \frac{1}{k'} \partial_a m' - \frac{\pi}{2} \frac{m'}{k'^2} \partial_a \frac{1}{k'} \\
 &= \pm \frac{\pi}{2} \frac{1}{k'} \frac{2R}{(a+R)^2} \\
 &= \pm \frac{\pi}{2} \frac{1}{k'} \frac{1}{2R}
 \end{aligned}$$

From Eq.(A8), we have $\lim_{m \rightarrow 1} \zeta = \pm 2R \frac{k'}{k}$. Consequently, we get for $\zeta < 0$:

$$\lim_{m \rightarrow 1} \zeta k \partial_a m'^2 \mathbf{\Pi}(m, k) = \pm \frac{\pi}{2}, \quad (\text{C4})$$

meaning that the jump in the derivative of $\zeta \mathbf{H}$ amounts to π when a increases and crosses the radius $a = R$. Since the Green kernel contains the difference $\zeta_+ \mathbf{\Pi}(m, k_+) - \zeta_- \mathbf{\Pi}(m, k_-)$, the jump is in fact 2π in total (see for instance Fig. 5, point A), except for a point located on the boundary ($\partial\Omega$) (i.e. if $Z = z_{\pm}(a)$), then it is only π . This is always true except for $\zeta = 0$. In this case, the jump disappears and we have:

$$m' \mathbf{\Pi}(m, m) \rightarrow \mathbf{E}(m) \quad (\text{C5})$$

which is perfectly continuous.

APPENDIX D: LONG-RANGE BEHAVIOR FOR THE EXACT POTENTIAL

At large distance from the body, we have

$$k \sim \frac{2\sqrt{aR}}{r} \rightarrow 0, \quad (\text{D1})$$

and so the behavior of the elliptic integrals is easily deduced. In particular, we have (Gradshteyn & Ryzhik 1965):

$$\begin{cases}
 \mathbf{K}(k) \sim \frac{\pi}{2} \left(1 + \frac{k^2}{4}\right), \\
 \mathbf{E}(k) \sim \frac{\pi}{2} \left(1 - \frac{k^2}{4}\right), \\
 \mathbf{\Pi}(m, k) \sim \frac{\pi}{2} \left[1 + \frac{1}{2} \left(m^2 - \frac{k^2}{2}\right)\right].
 \end{cases} \quad (\text{D2})$$

We then get:

$$\begin{aligned}
 -2G \int \rho(a) da \sqrt{\frac{a}{R}} \int k \mathbf{E}(k) d\zeta &\sim -4\pi G \frac{1}{r} \int \rho(a) h(a) da \\
 &\sim -\frac{GM}{r} \quad (\text{D3})
 \end{aligned}$$

which is the expected result. It can be checked that the contribution due to the \mathbf{H} -function is much smaller and behaves like k^3 . Actually, we find:

$$\begin{aligned}
 \zeta_{\pm} \mathbf{H}(m, k_{\pm}) &\sim \zeta_{\pm} k_{\pm} \frac{\pi}{2} \left[\frac{k_{\pm}^2}{2} - \frac{1}{2} \left(m^2 + \frac{k_{\pm}^2}{2}\right) (1 - m^2) + m^2 \right] \\
 &\sim \zeta_{\pm} k_{\pm} \frac{\pi}{4} (1 + m^2) \left(m^2 + \frac{k_{\pm}^2}{2}\right). \quad (\text{D4})
 \end{aligned}$$

As k_{\pm}^2 et m^2 are of the same order, $\zeta_{\pm} \mathbf{H}(m, k_{\pm})$ behaves like k_{\pm}^3 .

APPENDIX E: LONG-RANGE BEHAVIOR FOR THE APPROXIMATE POTENTIAL

The modulus k_{\pm} can be approximated as follows:

$$k_{\pm} \sim \frac{2\sqrt{aR}}{r} \left(1 - \frac{aR + Zz_{\pm}}{r^2}\right), \quad (\text{E1})$$

therefore the mean value \tilde{k} becomes:

$$\begin{aligned}
 \tilde{k} &\sim \frac{2\sqrt{aR}}{r} \left[1 - \frac{aR + (z_+ + z_-)Z}{r^2}\right] \\
 &\sim \frac{2\sqrt{aR}}{r} \left(1 - \frac{aR}{r^2}\right) \quad (\text{E2})
 \end{aligned}$$

We then get for \mathbf{T}_1 :

$$\begin{aligned}
 \mathbf{T}_1(\tilde{k})(\zeta_+ - \zeta_-) &\sim \frac{\pi}{2} h \tilde{k}^3 \\
 &\sim 4\pi h \frac{\sqrt{aR}^3}{r^3} \left(1 - \frac{aR}{r^2}\right)^3. \quad (\text{E3})
 \end{aligned}$$

Regarding the second term, we have:

$$\mathbf{T}_2(\tilde{k}) \sim \frac{\pi}{2} \left(1 - \frac{3}{4} \tilde{k}^2\right), \quad (\text{E4})$$

and

$$\int k d\zeta \sim k\zeta. \quad (\text{E5})$$

This order is sufficient. We then find:

$$\mathbf{T}_2(\tilde{k}) \int k d\zeta \sim -\pi \tilde{k} h \left(1 - \frac{3}{4} \tilde{k}^2\right) \quad (\text{E6})$$

and we see that this second term dominates over the first one. We then get:

$$\begin{aligned}
 -2G \int \rho(a) da \sqrt{\frac{a}{R}} \int k \mathbf{E}(k) d\zeta &\sim -4\pi G \frac{1}{r} \int \rho(a) h(a) da \\
 &\sim \frac{GM}{r} \quad (\text{E7})
 \end{aligned}$$